Processing of the ENDF/B-VIII.0β6 Neutron Cross-Section Data Library and Testing with Critical Benchmarks, Oktavian Shielding Benchmarks and the Doppler Reactivity Defect Benchmarks

KABACH Ouadie[1*], CHETAINE Abdelouahed[1], DARIF Abdelaziz[1], JALIL Abdelhamid[1], SAIDI Abdelmajid[1], BENCHRIF Abdelfettah[2] and AMSIL Hamid[2]

[1)] Mohammed V University, Faculty of Science, Nuclear Reactor and Nuclear Security Group Energy Centre, Physics Department, 4 Avenue Ibn Battouta B.P. 1014 RP, Rabat 10000, Morocco.

[2)] National Centre of Sciences, Energy and Nuclear Techniques (CNESTEN/CENM), POB 1382, Rabat, Morocco.

[*]**Corresponding author at**: University Mohamed V, Faculty of Science, Rabat Morocco.
Tel : +212 619262400. E-mail: ouadie.kabach10@gmail.com

Abstract

The recent release of ENDF/B-VIII.0β6 neutron cross-section data library has been processed and tested using benchmark calculations. The computations were performed with the NJOY2016 processing code and the MCNP(X) continuous energy Monte Carlo neutronics code. Three types of benchmark calculations were done: criticality safety benchmarks, Octavian shielding benchmarks and the Doppler reactivity defect benchmarks. For criticality benchmarks, the study has been conducted through the calculations for thirty-one criticality benchmarks taken from the *International Handbook of Criticality Safety Benchmark* (ICSBEP). For fusion shielding, many benchmarks were based on IAEA specifications for the Oktavian experiments for Al, Co, Cr, Cu, LiF, Mn, Mo, Nb, Si, Ti, W and Zr. For Doppler-Defect benchmarks, three fuel types were dealt: enriched uranium, Reactor-Recycle MOX, and Weapons-Grade MOX by varying enrichments or MOX contents. The obtained results were compared with the ENDF/B-VI.8, ENDF/B-VII.0, ENDF/B-VII.1, ENDF/B-VIII.0β4, ENDF/B-VIII.0β5 (*also processed using NJOY2016*) data libraries and the published values.

Keywords: ENDF/B-VIII.0β6, Critical, Oktavian Shielding, Doppler Defect, Benchmarks, MCNP(X), NJOY2016, Validation.

1. Introduction

The nuclear community needs benchmarks as tool to check various purposes and the availability of suitable experimental data. These data are fundamental to ensure that modelling tools meet the requirements of nuclear industry. Basically, they are used for: validation of nuclear cross-section data and libraries, validation of nuclear codes and models used, also we can use benchmarks for training users through benchmarking and code comparison exercises.

In order to be relevant, the definition of a benchmark has to be accurate and detailed enough to enable an unambiguous calculation. Errors or inaccuracies in cross-section or in

computational procedures lead to a calculation of a benchmark that disagrees with the experimentally measured benchmark. In this paper, the main objective is to validate the recent release of ENDF/B-VIII.0β6 neutron cross-section data library [1]. The evaluated nuclear ENDF/B-VIII.0β6 data library was released in December 15, 2017. The main revised data from the ENDF/B-VIII.0β6 are in the U.S. Cross Section Evaluation Working Group (CSEWG) web site [1]. To validate some of these data, three series of benchmark calculations were performed. The benchmark testing is carried out with a 31 different criticality data contained in the international handbook of evaluated criticality safety benchmark experiments (ICSBEP) [2], 12 Octavian Shielding Benchmarks from the IAEA web site [3] and Doppler-Defect benchmarks from [4]. The adequate MCNP(X) [5] calculations based on ENDF/B-VI.8, ENDF/B-VII.0 ENDF/B-VII.1, ENDF/B-VIII.0β4 and ENDF/B-VIII.0β5 [6] have also been done and compared with measurements. The ACE libraries used in the calculations were prepared with the LANL nuclear data processing system NJOY2016 [7].

2. Calculation tools and methods

2.1. Nuclear Data Processing converted from evaluated nuclear data to ACE format

The nuclear data evaluations are physical representations of the data encoded in the above-described unified computer-readable format called ENDF-6. They need to be converted into suitable forms for applications, such as transport or activation-transmutation calculations using multi-group, pointwise, deterministic or Monte Carlo techniques. In this paper, the ENDF files were processed using NJOY2016 for all isotopes to create ACE formatted files useful for applications calculations and compatible with MCNP code. All ENDF files were processed using exactly the same NJOY input, using the sequence of NJOY modules shown schematically in **Fig.1**.

In the NJOY [7], **MODER** is used to convert binary-to-ASCII or ASCII-to-binary mode, **RECONR** is used to reconstruct resonance cross-section from resonance parameters, the cross-section accuracy in this module is of the order of 0.5% (err = 0.005). **BROADR** is used to generate Doppler-broadened cross-section, the cross-section accuracy in this module is of the order of 0.5% (err = 0.005). **HEATR** is used to generate point-wise heat production cross-sections and radiation damage energy production for the specified reactions. **GASPR** is used to add gas production reactions. **THERMR** is used to generate point-wise neutron scattering cross-sections in the thermal energy range. **PURR** is used to produce probability tables for considering the self-shielding effects for MCNP. **ACER** is used to prepare libraries in ACE format for MCNP. Apart from the mentioned modules, there are a number of distinct modules used to verify the produced neutron cross-sections, ACER is capable of making a series of consistency checks and produces several plot files.

The thermal scattering [8] data were used for H in H_2O processed at 293.6 K and 600K, H in CH_2, graphite and Be in Beryllium metal, the data were processed at room temperature, which in some cases implied 293.6 K and in other 296 K, as necessary for consistency with the data file. These thermal scattering data are essential to accurately model the neutron interactions at energies below then 4eV.

2.2. MCNP(X) v2.6.0

In this study, the MCNP(X) v2.6.0 calculations were carried out with an HP EliteBook 8560 workstation Intel® i7 CPU 2.20 GHz, 8 cores, 8 Gb RAM and 6 Mb Cache Memory under Win 10 system and using MPICH2 [9]. The keff parameter of criticality and Doppler Defect calculations were performed using these six libraries with 600 iterations on a nominal

source size of 60000 particles per cycle in order to decrease statistical error estimates, initial 100 cycles were skipped to insure homogeneous neutrons source distribution. For Oktavian benchmarks, 500000000 neutron histories were run.

3. Criticality benchmarks

3.1. Brief description of the criticality benchmarks [10]

In this paper, all criticality benchmarks were taken from OECD-NEA project ICSBEP [2]. In Ref. [2], the evaluations in this Handbook are defined using an XXX-YYY-ZZZ-aaa.b nomenclature system. The XXX designator defines the fuel system and includes Pu for ^{239}Pu fuelled systems, and HEU, IEU and LEU for highly enriched, intermediate-enriched and low-enriched ^{235}U fuel systems. Highly enriched systems contain at least 90% ^{235}U, low-enriched systems contain less than 10% ^{235}U while intermediate-enriched systems cover the intervening range. Other XXX designators include U233 for ^{233}U fuelled systems and MIX which is used for systems with both ^{235}U and ^{239}Pu. The YYY designator defines the chemical form of the fuel, with MET meaning a metal system, SOL being a solution and COMP a compound. ZZZ is used to define the average fission energy. FAST is used when more than 50% of the fissions occur above 100 KeV and THERM is used if more than 50% of the fissions occur below 0.625 eV. INTER is used when 50% or more of the fissions occur between these energy limits, and MIXED is used when no energy interval has 50% or more fissions. Finally, aaa.b is a simple numerical index, and .b represents one of the individual case numbers when multiple experiments are described in a single evaluation.

3.2. Results of criticality calculations

The results of MCNP(X) keff calculations with ENDF/B-VI.8[11], ENDF/B-VII.0[11], ENDF/B-VII.1[11], ENDF/B-VIII.0β4[11], ENDF/B-VIII.0β5 and ENDF/B-VIII.0β6 data libraries for the suite of benchmarks as well as the benchmark keff values are given in **Table 1** and illustrated in **Fig. 2**.**Table 2** provides the average value of C/E-1 ('E' is the expected or benchmark value and 'C' is the calculated value) and its uncertainty for each of the benchmark systems. These average values and their uncertainties are also summarized in **Fig.3**.

Results using the new ENDF/B-VIII.0β6 data library have been improved in the fourteen among the thirty-one benchmark systems because deviations from the benchmark values are <100 pcm. In addition, the values of C/E-1 deviate from the benchmark values by > 1000 pcm in just two cases. It should be pointed out that the largest deviations have been observed for the U233-SOL-INTER-001-case-1 benchmark for all libraries except the ENDF/B-VII.0, ENDF/B-VIII.0β5 and ENDF/B-VIII.0β6 libraries. In the "U233-SOL-INTER-001-case-1" benchmark, Beryllium (Be) is employed as the reflector. In the latter library, the Be data are significantly more accurate than those of the ENDF/B-VIII.0β4 library discussed in [11] since deviations from the benchmark values are < 2000 pcm for this benchmark.

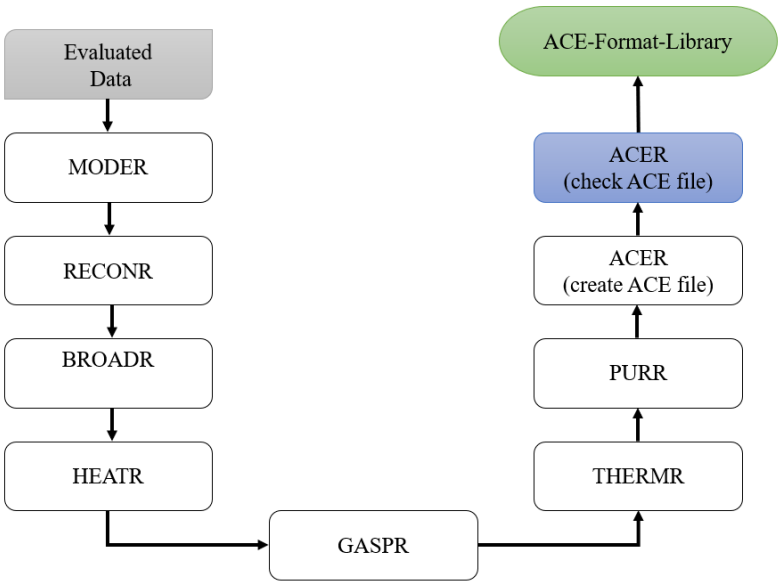

Fig.1. Flow chart of nuclear data processing code NJOY2016.

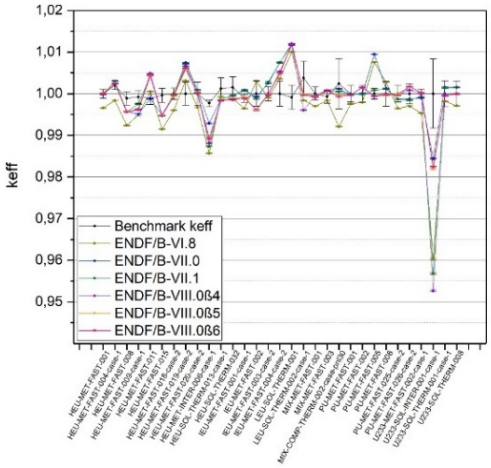

Fig.2. MCNP(X) calculations of keff values and its uncertainty with six data libraries and benchmark keff.

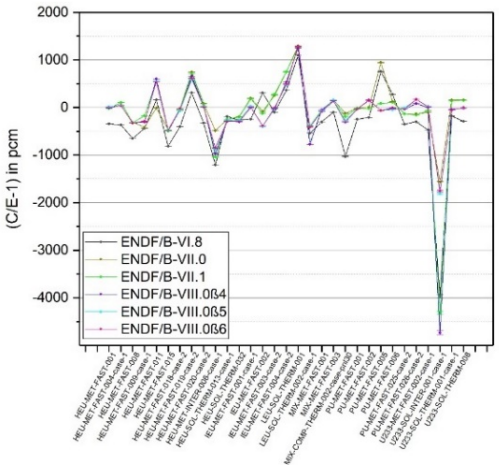

Fig.3. Value of $\frac{C}{E} - 1$ and its uncertainty (in pcm) for all benchmark cases.

Table 1. MCNP(X) calculations of keff values with six data libraries and benchmark keff.

Case Name	Benchmark keff	ENDF/B-VI.8	ENDF/B-VII.0	ENDF/B-VII.1	ENDF/B-VIII.0β4	ENDF/B-VIII.0β5	ENDF/B-VIII.0β6
HEU-MET-FAST-001	1.00000 ± 0.00100	0.99656 ± 0.00010	0.99985 ± 0.00010	0.99978 ± 0.00010	0.99994 ± 0.00010	1.00014 ± 0.00011	1.00003 ± 0.00011
HEU-MET-FAST-004-case-1	1.00200 ± 0.00100	0.99833 ± 0.00010	1.00302 ± 0.00010	1.00305 ± 0.00010	1.00250 ± 0.00010	1.00249 ± 0.00015	1.00242 ± 0.00014
HEU-MET-FAST-008	0.99890 ± 0.00160	0.99240 ± 0.00010	0.99577 ± 0.00010	0.99573 ± 0.00010	0.99562 ± 0.00010	0.99570 ± 0.00010	0.99567 ± 0.00011
HEU-MET-FAST-009-case-1	0.99920 ± 0.00150	0.99484 ± 0.00010	0.99507 ± 0.00010	0.99749 ± 0.00010	0.99615 ± 0.00010	0.99629 ± 0.00012	0.99627 ± 0.00012
HEU-MET-FAST-011	0.99890 ± 0.00150	1.00050 ± 0.00010	0.99881 ± 0.00010	1.00437 ± 0.00010	1.00489 ± 0.00010	1.00445 ± 0.00014	1.00431 ± 000014
HEU-MET-FAST-015	0.99960 ± 0.00170	0.99146 ± 0.00010	0.99491 ± 0.00010	0.99466 ± 0.00010	0.99478 ± 0.00010	0.99488 ± 0.00011	0.99479 ± 0.00012
HEU-MET-FAST-018-case-2	1.00000 ± 0.00140	0.99599 ± 0.00010	0.99971 ± 0.00010	0.99959 ± 0.00010	0.99936 ± 0.00010	0.99938 ± 0.00011	0.99973 ± 0.00011
HEU-MET-FAST-019-case-2	1.00000 ± 0.00280	1.00310 ± 0.00010	1.00746 ± 0.00010	1.00713 ± 0.00010	1.00658 ± 0.00010	1.00585 ± 0.00011	1.00612 ± 0.00011
HEU-MET-FAST-020-case-2	1.00000 ± 0.00280	0.99677 ± 0.00010	1.00087 ± 0.00010	1.00078 ± 0.00010	1.00031 ± 0.00010	1.00025 ± 0.00012	1.00013 ± 0.00012
HEU-MET-INTER-006-case-1	0.99770 ± 0.00080	0.98567 ± 0.00010	0.99286 ± 0.00010	0.98734 ± 0.00010	0.98805 ± 0.00010	0.98905 ± 0.00014	0.98924 ± 0.00014
HEU-SOL-THERM-013-case-1	1.00120 ± 0.00260	0.99930 ± 0.00010	0.99872 ± 0.00010	0.99872 ± 0.00010	0.99844 ± 0.00010	0.99849 ± 0.00011	0.99830 ± 0.00011
HEU-SOL-THERM-032	1.00150 ± 0.00260	0.99880 ± 0.00010	0.99956 ± 0.00010	0.99951 ± 0.00010	0.99850 ± 0.00010	0.99877 ± 0.00007	0.99861 ± 0.00007
IEU-MET-FAST-001-case-1	0.99890 ± 0.00100	0.99645 ± 0.00010	1.00087 ± 0.00010	1.00073 ± 0.00010	0.99901 ± 0.00010	0.99914 ± 0.00011	0.99888 ± 0.00011
IEU-MET-FAST-002	1.00000 ± 0.00300	1.00305 ± 0.00010	0.99920 ± 0.00010	0.99876 ± 0.00010	0.99613 ± 0.00010	0.99602 ± 0.00010	0.99611 ± 0.00010
IEU-MET-FAST-003-case-2	1.00000 ± 0.00170	0.99902 ± 0.00010	1.00251 ± 0.00010	1.00277 ± 0.00010	0.99968 ± 0.00010	0.99984 ± 0.00010	0.99991 ± 0.00010
IEU-MET-FAST-004-case-2	1.00000 ± 0.00300	1.00362 ± 0.00010	1.00747 ± 0.00010	1.00751 ± 0.00010	1.00533 ± 0.00010	1.00474 ± 0.00011	1.00494 ± 0.00011
LEU-SOL-THERM-001	0.99910 ± 0.00290	1.01004 ± 0.00010	1.01201 ± 0.00010	1.01172 ± 0.00010	1.01164 ± 0.00010	1.01193 ± 0.00015	1.01194 ± 0.00014
LEU-SOL-THERM-002-case-1	1.00380 ± 0.00400	0.99838 ± 0.00010	0.99993 ± 0.00010	0.99992 ± 0.00010	0.99605 ± 0.00010	0.99987 ± 0.00010	0.99969 ± 0.00010
MIX-MET-FAST-001	1.00000 ± 0.00160	0.99698 ± 0.00010	0.99947 ± 0.00010	0.99952 ± 0.00010	0.99951 ± 0.00010	0.99929 ± 0.00011	0.99917 ± 0.00010
MIX-MET-FAST-003	0.99930 ± 0.00160	0.99833 ± 0.00010	1.00087 ± 0.00010	1.00067 ± 0.00010	1.00073 ± 0.00010	1.00086 ± 0.00011	1.00065 ± 0.00011
MIX-COMP-THERM-002-case-pnl30	1.00240 ± 0.00600	0.99207 ± 0.00010	1.00117 ± 0.00010	1.00049 ± 0.00010	0.99957 ± 0.00010	0.99953 ± 0.00014	0.99932 ± 0.00014
PU-MET-FAST-001	1.00000 ± 0.00200	0.99752 ± 0.00010	0.99985 ± 0.00010	0.99987 ± 0.00010	0.99974 ± 0.00010	0.99969 ± 0.00010	0.99969 ± 0.00010
PU-MET-FAST-002	1.00000 ± 0.00200	0.99792 ± 0.00010	1.00004 ± 0.00010	0.99981 ± 0.00010	1.00149 ± 0.00010	1.00156 ± 0.00010	1.00156 ± 0.00010
PU-MET-FAST-005	1.00000 ± 0.00130	1.00753 ± 0.00010	1.00943 ± 0.00010	1.00085 ± 0.00010	0.99940 ± 0.00010	0.99940 ± 0.00011	0.99940 ± 0.00011
PU-MET-FAST-006	1.00000 ± 0.00300	1.00275 ± 0.00010	1.00123 ± 0.00010	1.00110 ± 0.00010	0.99970 ± 0.00010	0.99955 ± 0.00012	0.99991 ± 0.00013
PU-MET-FAST-025-case-2	1.00000 ± 0.00200	0.99649 ± 0.00010	0.99868 ± 0.00010	0.99867 ± 0.00010	0.99967 ± 0.00010	0.99988 ± 0.00011	0.99968 ± 0.00011
PU-MET-FAST-026-case-2	1.00000 ± 0.00240	0.99700 ± 0.00010	0.99866 ± 0.00010	0.99844 ± 0.00010	1.00083 ± 0.00010	1.00169 ± 0.00013	1.00170 ± 0.00011
U233-MET-FAST-002-case-1	1.00000 ± 0.00100	0.99530 ± 0.00010	0.99897 ± 0.00010	0.99933 ± 0.00010	1.00003 ± 0.00010	1.00025 ± 0.00011	1.00019 ± 0.00011
U233-SOL-INTER-001-case-1	1.00000 ± 0.00830	0.96033 ± 0.00020	0.98440 ± 0.00020	0.95684 ± 0.00020	0.95268 ± 0.00010	0.98190 ± 0.00020	0.98246 ± 0.00019
U233-SOL-THERM-001-case-1	1.00000 ± 0.00310	0.99818 ± 0.00010	1.00157 ± 0.00010	1.00139 ± 0.00010	0.99964 ± 0.00010	0.99950 ± 0.00011	0.99948 ± 0.00010
U233-SOL-THERM-008	1.00000 ± 0.00290	0.99708 ± 0.00010	1.00157 ± 0.00010	1.00149 ± 0.00010	0.99987 ± 0.00010	0.99994 ± 0.00007	0.99998 ± 0.00007

Table 2. Value of $\frac{C}{E} - 1$ and its uncertainty (in pcm) for all benchmark cases.

Case Name	ENDF/B-VI.8	ENDF/B-VII.0	ENDF/B-VII.1	ENDF/B-VIII.0β4	ENDF/B-VIII.0β5	ENDF/B-VIII.0β6
HEU-MET-FAST-001	-344.0000 ± 0.3457	-15.0000 ± 0.0151	-22.0000 ± 0.0221	-6.0000 ± 0.0060	14.0000 ± 0.0141	3.0000 ± 0.0030
HEU-MET-FAST-004-case-1	-366.2675 ± 0.3674	101.7964 ± 0.1021	104.7904 ± 0.1051	49.9002 ± 0.0500	48.9022 ± 0.0494	41.9162 ± 0.0422
HEU-MET-FAST-008	-650.7158 ± 1.0444	-313.3447 ± 0.5029	-317.3491 ± 0.5093	-328.3612 ± 0.5270	-320.3524 ± 0.5141	-323.3557 ± 0.5192
HEU-MET-FAST-009-case-1	-436.3491 ± 0.6565	-413.3307 ± 0.6219	-171.1369 ± 0.2575	-305.2442 ± 0.4593	-291.2330 ± 0.4386	-293.2346 ± 0.4416
HEU-MET-FAST-011	160.1762 ± 0.2411	-9.0099 ± 0.0136	547.6024 ± 0.8241	599.6596 ± 0.9025	555.6112 ± 0.8379	541.5958 ± 0.8168
HEU-MET-FAST-015	-814.3257 ± 1.3873	-469.1877 ± 0.7993	-494.1977 ± 0.8419	-482.1929 ± 0.8215	-472.1889 ± 0.8047	-481.1925 ± 0.8204
HEU-MET-FAST-018-case-2	-401.0000 ± 0.5628	-29.0000 ± 0.0407	-41.0000 ± 0.0575	-64.0000 ± 0.0898	-62.0000 ± 0.0871	-27.0000 ± 0.0379
HEU-MET-FAST-019-case-2	310.0000 ± 0.8685	746.0000 ± 2.0901	713.0000 ± 1.9977	658.0000 ± 1.8436	585.0000 ± 1.6392	612.0000 ± 1.7149
HEU-MET-FAST-020-case-2	-323.0000 ± 0.9050	87.0000 ± 0.2438	78.0000 ± 0.2185	31.0000 ± 0.0869	25.0000 ± 0.0701	13.0000 ± 0.0364
HEU-MET-INTER-006-case-1	-1205.7733 ± 0.9746	-485.1158 ± 0.3920	-1038.3883 ± 0.8392	-967.2246 ± 0.7817	-866.9941 ± 0.7059	-847.9503 ± 0.6904
HEU-SOL-THERM-013-case-1	-189.7723 ± 0.4932	-247.7028 ± 0.6437	-247.7028 ± 0.6437	-275.6692 ± 0.7164	-270.6751 ± 0.7035	-289.6524 ± 0.7529
HEU-SOL-THERM-032	-269.5956 ± 0.7004	-193.7094 ± 0.5033	-198.7019 ± 0.5162	-299.5507 ± 0.7782	-272.5911 ± 0.7079	-288.5671 ± 0.7494
IEU-MET-FAST-001-case-1	-245.2698 ± 0.2468	197.2169 ± 0.1984	183.2015 ± 0.1843	11.0121 ± 0.0111	24.0264 ± 0.0242	-2.0022 ± 0.0020
IEU-MET-FAST-002	305.0000 ± 0.9155	-80.0000 ± 0.2401	-124.0000 ± 0.3722	-387.0000 ± 1.1616	-398.0000 ± 1.1947	-389.0000 ± 1.1677
IEU-MET-FAST-003-case-2	-98.0000 ± 0.1669	251.0000 ± 0.4274	277.0000 ± 0.4717	-32.0000 ± 0.0545	-16.0000 ± 0.0272	-9.0000 ± 0.0153
IEU-MET-FAST-004-case-2	362.0000 ± 1.0866	747.0000 ± 2.2422	751.0000 ± 2.2542	533.0000 ± 1.5999	474.0000 ± 1.4229	494.0000 ± 1.4830
LEU-SOL-THERM-001	1094.9855 ± 3.1802	1292.1629 ± 3.7528	1263.1368 ± 3.6685	1255.1296 ± 3.6453	1284.1557 ± 3.7323	1285.1566 ± 3.7345
LEU-SOL-THERM-002-case-1	-539.9482 ± 2.1523	-385.5350 ± 1.5368	-386.5312 ± 1.5408	-772.0661 ± 3.0775	-391.5122 ± 1.5606	-409.4441 ± 1.6321
MIX-MET-FAST-001	-302.0000 ± 0.4841	-53.0000 ± 0.0850	-48.0000 ± 0.0769	-49.0000 ± 0.0786	-71.0000 ± 0.1139	-83.0000 ± 0.1331
MIX-MET-FAST-003	-97.0679 ± 0 .1557	157.1100 ± 0.2520	137.0960 ± 0.2199	143.1002 ± 0.2296	156.1092 ± 0.2505	135.0946 ± 0.2168
MIX-COMP-THERM-002-case-pnl30	-1030.5267 ± 6.1692	-122.7055 ± 0.7346	-190.5427 ± 1.1407	-282.3224 ± 1.6901	-282.3224 ± 1.7142	-307.2626 ± 1.8397
PU-MET-FAST-001	-248.0000 ± 0.4966	-15.0000 ± 0.0300	-13.0000 ± 0.0260	-26.0000 ± 0.0521	-31.0000 ± 0.0621	-31.0000 ± 0.0621
PU-MET-FAST-002	-208.0000 ± 0.4165	4.0000 ± 0.0080	-19.0000 ± 0.0380	149.0000 ± 0.2984	156.0000 ± 0.3124	156.0000 ± 0.3124
PU-MET-FAST-005	753.0000 ± 0.9817	943.0000 ± 1.2295	85.0000 ± 0.1108	-60.0000 ± 0.0782	-60.0000 ± 0.0783	-60.0000 ± 0.0783
PU-MET-FAST-006	275.0000 ± 0.8255	123.0000 ± 0.3692	110.0000 ± 0.3302	-30.0000 ± 0.0901	-45.0000 ± 0.1351	-9.0000 ± 0.0270
PU-MET-FAST-025-case-2	-351.0000 ± 0.7029	-132.0000 ± 0.2643	-133.0000 ± 0.2663	-33.0000 ± 0.0661	-12.0000 ± 0.0240	-32.0000 ± 0.0641
PU-MET-FAST-026-case-2	-300.0000 ± 0.7206	-134.0000 ± 0.3219	-156.0000 ± 0.3747	83.0000 ± 0.1994	169.0000 ± 0.4062	170.0000 ± 0.4084
U233-MET-FAST-002-case-1	-470.0000 ± 0.4724	-103.0000 ± 0.1035	-67.0000 ± 0.0673	3.0000 ± 0.0030	25.0000 ± 0.0252	19.0000 ± 0.0191
U233-SOL-INTER-001-case-1	-3967.0000 ± 32.9365	-1560.0000 ± 12.9519	-4316.0000 ± 35.8342	-4732.0000 ± 39.2882	-1810.0000 ± 15.0275	-1754.0000 ± 4.5622
U233-SOL-THERM-001-case-1	-182.0000 ± 0.5645	157.0000 ± 0.4870	139.0000 ± 0.4311	-36.0000 ± 0.1117	-50.0000 ± 0.1551	-52.0000 ± 0.1613
U233-SOL-THERM-008	-292.0000 ± 0.8473	157.0000 ± 0.4556	149.0000 ± 0.4324	-13.0000 ± 0.0377	-6.0000 ± 0.0174	-2.0000 ± 0.0058

4. Okatvian shielding benchmarks

4.1. Brief description of Okatvian shielding benchmarks

The Oktavian benchmark specifications are given on the IAEA web site [3]. The leakage current spectra from spherical piles were measured with the time-of flight (TOF) technique at the Octavian DT neutron source facility in Osaka University. At the centre of a pile, a 14 MeV D-T neutron source was located. The piles were made by filling spherical vessels with sample powder or flakes of Al, Co, Cr, Cu, LiF, Mn, Mo, Nb, Si, Ti, W and Zr. The material densities and outer diameters of the vessels are summarized in **Table 3** and the experimental arrangement is shown in **Fig. 4.**

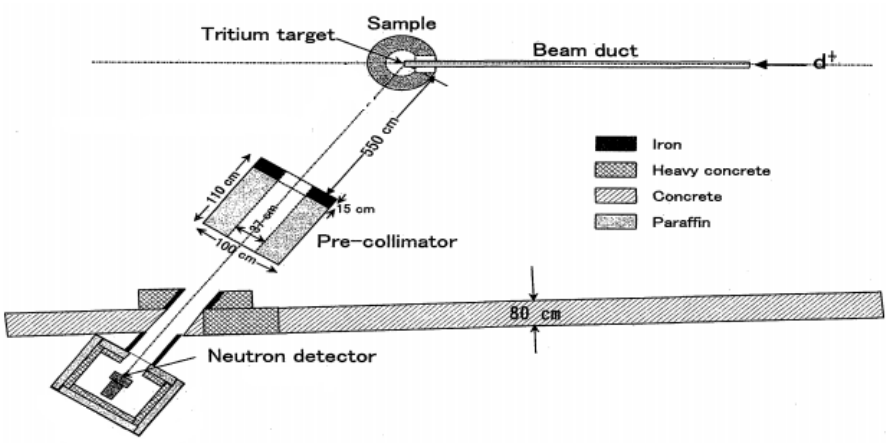

Fig.4. Experimental arrangement at Oktavian [12].

Table 3. Material density and outer diameter of vessel [3].

Material		Apparent density (g/cm3)	Outer diameter of vessel (Cm)
Aluminium	Al	1.22	40
Cobalt	Co	1.94	40
Chromium	Cr	3.72	40
Copper	Cu	6.23	61
Lithium Fluoride	LiF	1.79	61
Manganese	Mn	4.37	61
Molybdenum	Mo	2.15	61
Niobium	Nb	4.39	28
Silicon	Si	1.29	60
Titanium	Ti	1.54	40
Tungsten	W	4.43	40
Zirconium	Zr	2.84	61

4.2. Results of Okatvian shielding calculations

In this section, we report the results of our calculations with ENDF/B-VIII.0β6, ENDF/B-VIII.0β5, ENDF/B-VIII.0β4, ENDF/B-VII.1, ENDF/B-VII.0 and ENDF/B-VI.8 libraries. These results are reported as graphs of the neutron spectrum, as well as C/E values

for the neutron spectrum for each specific energy region of 0.1 to 0.5 MeV, 0.5 to 1 MeV, 1 to 5 MeV, 5 to 10 MeV and > 10 MeV.

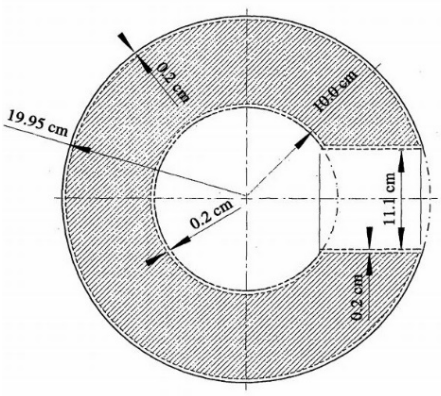

Fig.5. Schematic drawing of the Oktavian geometry for the Al benchmark.

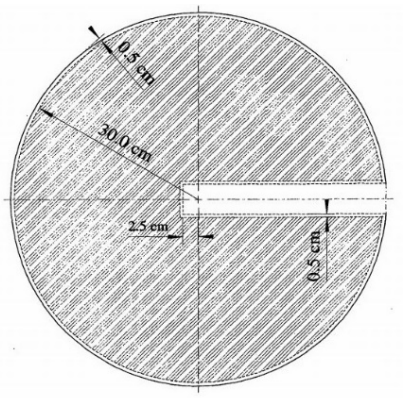

Fig.6. Schematic drawing of the Oktavian geometry for the Zr benchmark.

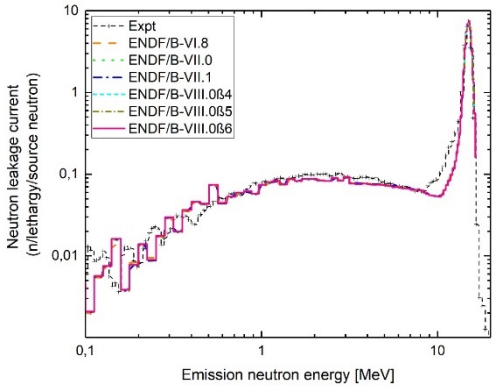

Fig.7. Measured and calculated leakage neutron spectrum for the
Oktavian Al benchmark.

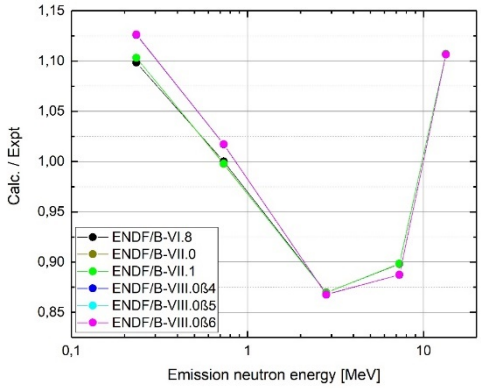

Fig.8. C/E values for the neutron spectrum of the Oktavian Al benchmark.

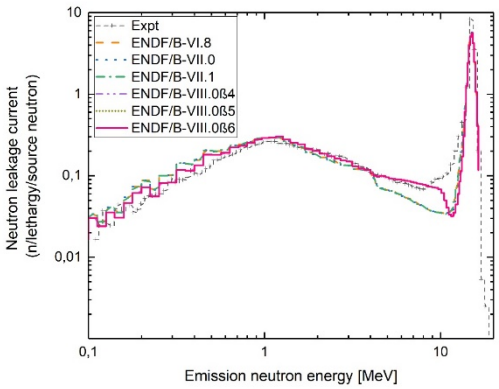

Fig.9. Measured and calculated leakage neutron spectrum for the
Oktavian Co benchmark.

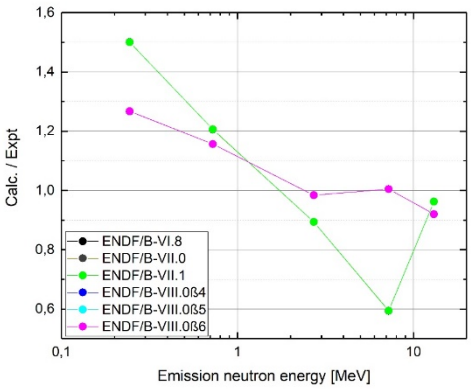

Fig.10. C/E values for the neutron spectrum of the Oktavian Co benchmark.

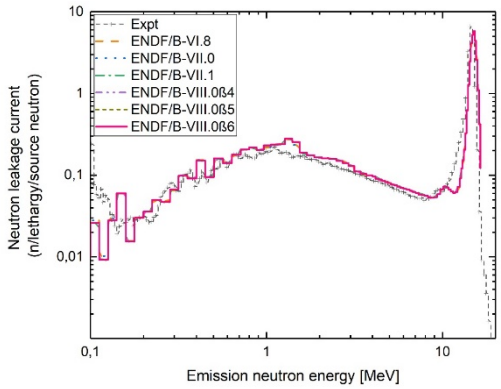

Fig.11. Measured and calculated leakage neutron spectrum for the Oktavian Cr benchmark.

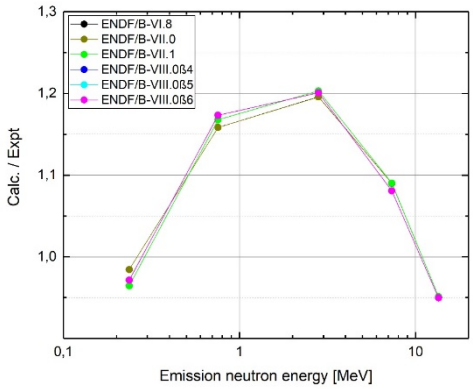

Fig.12. C/E values for the neutron spectrum of the Oktavian Cr benchmark.

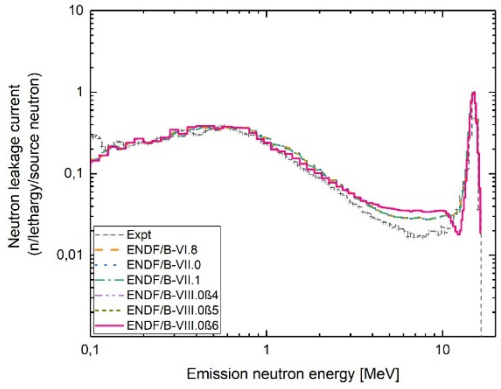

Fig.13. Measured and calculated leakage neutron spectrum for the Oktavian Cu benchmark.

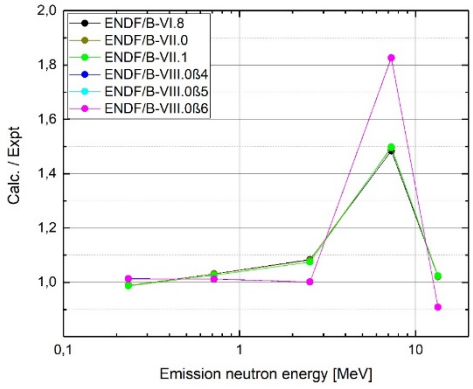

Fig.14. C/E values for the neutron spectrum of the Oktavian Cu benchmark.

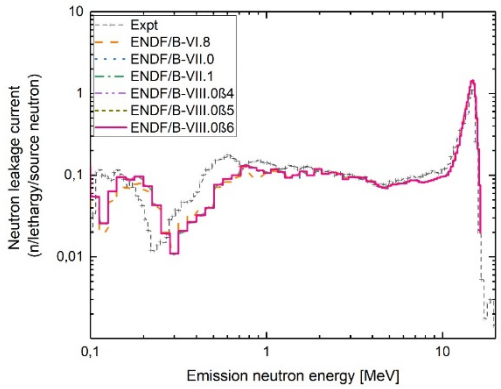

Fig.15. Measured and calculated leakage neutron spectrum for the Oktavian LiF benchmark.

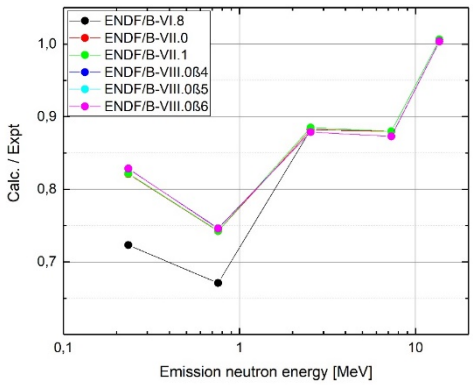

Fig.16. C/E values for the neutron spectrum of the Oktavian LiF benchmark.

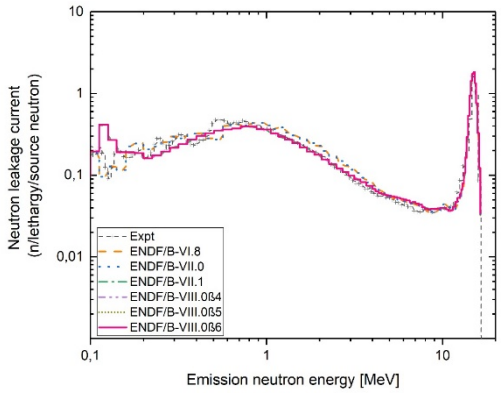

Fig.17. Measured and calculated leakage neutron spectrum for the Oktavian Mn benchmark.

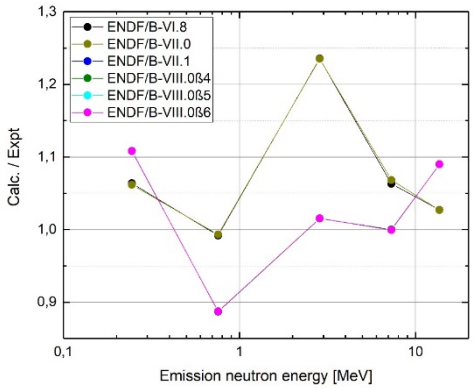

Fig.18. C/E values for the neutron spectrum of the Oktavian Mn benchmark.

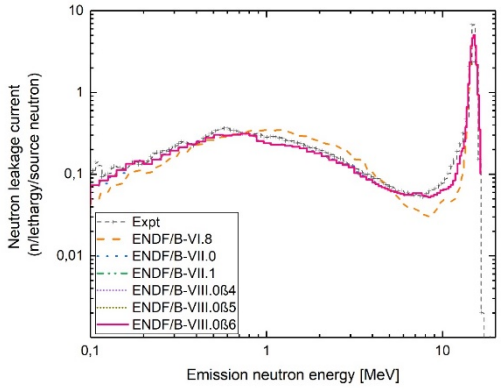

Fig.19. Measured and calculated leakage neutron spectrum for the Oktavian Mo benchmark.

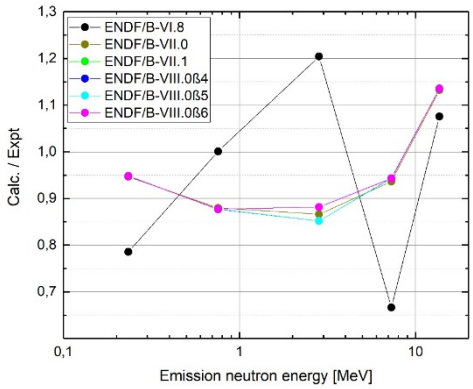

Fig.20. C/E values for the neutron spectrum of the Oktavian Mo benchmark.

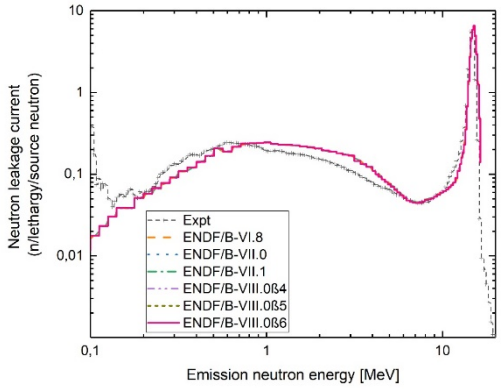

Fig.21. Measured and calculated leakage neutron spectrum for the Oktavian Nb benchmark.

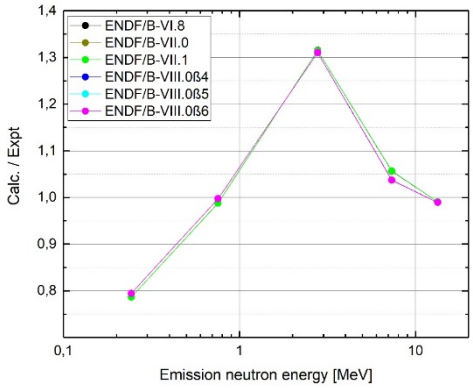

Fig.22. C/E values for the neutron spectrum of the Oktavian Nb benchmark.

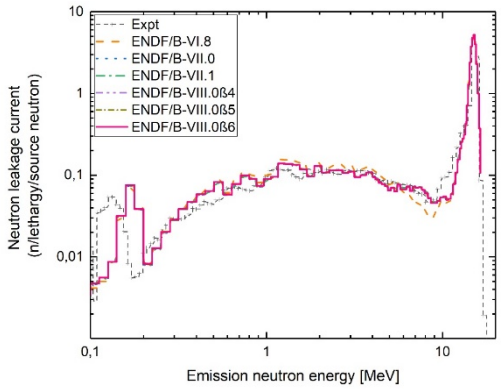

Fig.23. Measured and calculated leakage neutron spectrum for the
Oktavian Si benchmark.

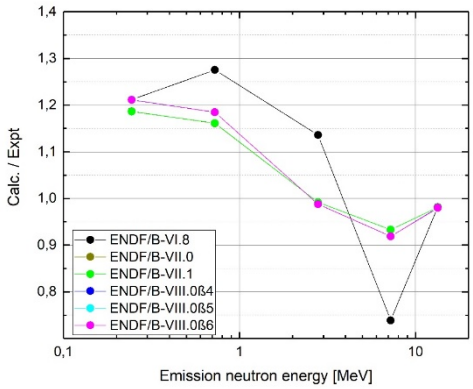

Fig.24. C/E values for the neutron spectrum of the Oktavian Si benchmark.

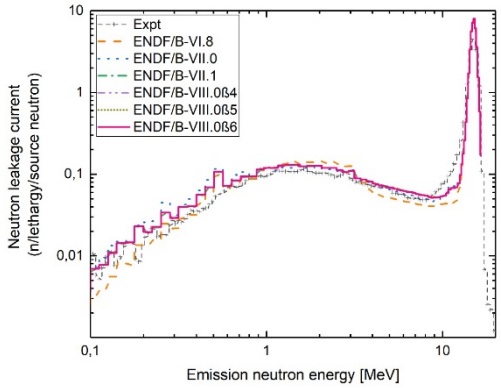

Fig.25. Measured and calculated leakage neutron spectrum for the
Oktavian Ti benchmark.

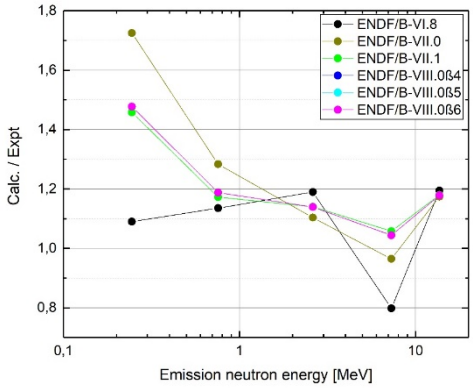

Fig.26. C/E values for the neutron spectrum of the Oktavian Ti benchmark.

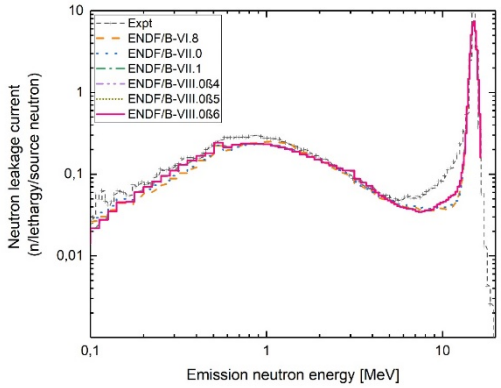

Fig.27. Measured and calculated leakage neutron spectrum for the
Oktavian W benchmark.

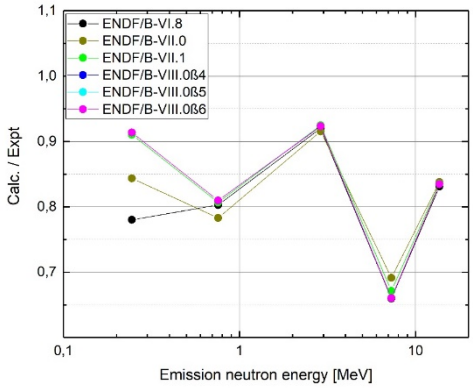

Fig.28. C/E values for the neutron spectrum of the Oktavian W benchmark.

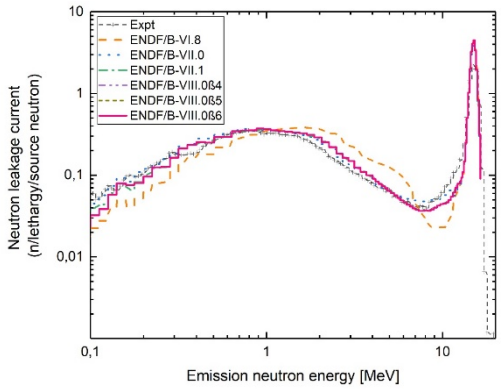

Fig.29. Measured and calculated leakage neutron spectrum for the Oktavian Zr benchmark.

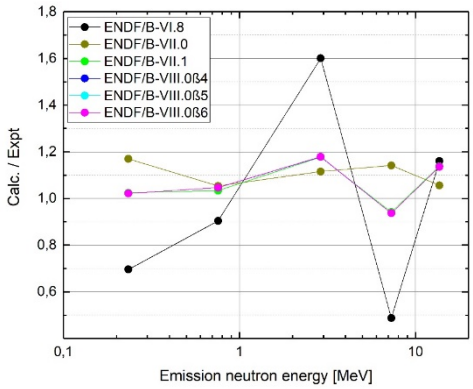

Fig.30. C/E values for the neutron spectrum of the Oktavian Zr benchmark.

Summary of Shielding Benchmarks Results: From the results of the Oktavian benchmarks described above, the following remarks can be underlined:

Oktavian Al benchmark: For each specific energy region, the calculated and measured values of the neutron spectra and the C/E values using the data of six libraries are illustrated in Figures 7 and 8, respectively. The calculation results demonstrate that all the libraries perform the same way including the new one. In addition, these results are generally good in the interval between 0.5 to 1 MeV.

Oktavian Co benchmark: Figures 9 and 10 indicate the experimental and calculated neutron spectra and the C/E for each specific energy region, respectively. The calculation results based on ENDF/B-VIII.0β6 data are closest to the values of benchmark in the range between 0.1 to 10 MeV.

Oktavian Cr benchmark: Figures 11 and 12 show the experimental and computational values of neutron spectra and the C/E values for each specific energy region, respectively. The calculation results using new ENDF/B-VIII.0β6 are almost the same as those obtained with the other libraries.

Oktavian Cu benchmark: The measured and calculated neutron spectra and the C/E for each specific energy region are shown in Figures 13 and 14, respectively. The calculation results with ENDF/B-VIII.0β6 data are improved between 0.1 to 5 MeV, but these results tend to be high in energy interval between 5 to 10 MeV.

Oktavian LiF benchmark: The experimental and computational values of neutron spectra and the C/E values for each specific energy region are presented in Figures 15 and 16, respectively. The calculation results show that all the libraries perform equally, except for ENDF/B-VI.8 data library. Note that these results are the best in the energy range between 10 to 20 MeV.

Oktavian Mn benchmark: Figures 17 and 18 give the measured and calculated neutron spectra and the C/E for each specific energy region, respectively. The calculation results using the new ENDF/B-VIII.0β6 data library are closest to the benchmark values in the interval

between 5 to 10 MeV, but this library was not improved in the other intervals. It can be seen that the ENDF/B-VII.0 library performs well between 0.1 to 1 MeV.

Oktavian Mo benchmark: Figures 19 and 20 summarize the measured and calculated values of neutron spectra and the C/E for each specific energy region, respectively. The calculation results indicate that all the libraries perform the same way, except ENDF/B-VI.8 which performs better between 0.5 to 1 MeV.

Oktavian Nb benchmark: The measured and calculated neutron spectra and the C/E for each specific energy region are illustrated in Figures 21 and 22, respectively. The calculation results show that all the libraries perform the same way. These results tend to be high between 1 to 5 MeV, but they are closest to benchmark values in both energy intervals 0.5 to 1 MeV and 5 to 20 MeV.

Oktavian Si benchmark: The experimental and calculated neutron spectra and the C/E for each specific energy region can be seen in Figures 23 and 24, respectively. The calculation results are generally identical for ENDF/B-VIII.0β6, ENDF/B-VII.0, ENDF/B-VII.1, ENDF/B-VIII.0β4 and ENDF/B-VIII.0β5. It is observed that these results are good between 1 to 20 MeV.

Oktavian Ti benchmark: The measured and computed neutron spectra and the C/E values for each specific energy region are summarized in Figures 25 and 26, respectively. The performed calculations demonstrate that the results are good from 0.1 to 1 MeV using ENDF/B-VI.8 and from 5 to 10 MeV with ENDF/B-VII.0. For the new ENDF/B-VIII.0β6 library, the results are located between those of the other libraries.

Oktavian W benchmark: Figures 27 and 28 show the measured and calculated values of neutron spectra and the C/E values for each specific energy region, respectively. From these Figures, it can be observed that all the libraries perform the same way between 0.5 to 20 MeV, but they perform poorly between 5 to 10 MeV.

Oktavian Zr benchmark: The experimental and computed neutron spectra and the C/E values for each specific energy region are shown in Figures 29 and 30, respectively. The new ENDF/B-VIII.0β6 library is better performing between 0.1 to 1 MeV. Furthermore, the results are closest to the benchmark values between 5 to 10 MeV.

From the results of this work, it could be noted that, on the one hand, the computed values using ENDF/B-VIII.0β6 for the Oktavian shielding benchmarks are generally good, but strong deviations from the benchmark values in some cases occur. In the other hand, there is little difference between the libraries for most of the calculations. As far as there are larger differences, in many cases this can likely be attributed to original nuclear data.

5. Doppler Benchmarks

5.1. Brief description of Doppler Reactivity Defect Benchmarks [4]

Doppler reactivity coefficient is defined as a relation between fuel temperature changes and reactivity changes in the nuclear reactor core. Doppler coefficient evaluation involves the study of reactivity change with respect to change in fuel temperature by keeping other parameters like moderator temperature, moderator density, boron concentration, xenon poisoning, burn-up, etc., constant, while changing fuel temperature from one to another.

Doppler reactivity coefficient needs to be known because the data generated are required in the analysis of nuclear reactor transients and the safety of reactor operation.

5.2. Benchmark specifications [13]

The geometry for the benchmark calculations is an infinite array of identical pin cells, infinite in length. The pin cell consists of a cylindrical fuel pin surrounded by a gap, zirconium cladding and borated water. The benchmark is a pair of calculations for hot zero power (HZP) and hot full power (HFP) for the infinite array of pin cells. At HZP, the temperature for the fuel, clad, and moderator is uniform at 600 K. At HFP, the clad and moderator temperature remains at 600 K and the temperature of the fuel is increased to 900 K. The Doppler defect is the calculated change in the reactivity between HFP and HZP.

The Doppler coefficient of reactivity is then determined as: $D_c = \frac{\Delta\rho}{\Delta T}$ and $\Delta\rho = \frac{k_{eff}^{HFP} - k_{eff}^{HZP}}{k_{eff}^{HFP} * k_{eff}^{HZP}}$

Pin Cell Dimensions:

Table 4. Pin cell dimensions for different temperatures.

Dimensions (Cm)	600K	900K
Radius of Fuel	0.39398	0.39433
Inner Radius of Clad	0.40226	0.40226
Outer Radius of Clad	0.45972	0.45972
Pitch	1.26678	1.26678

Fuel description:

The 16 types of fuel are considered, namely seven conventional UO_2 fuels with enrichment ranging from natural uranium to 5.0 wgt%, 5 Reactor-Recycle MOX fuels with enrichment ranging from 1.0 to 8.0 wgt% and 4 Weapons-Grade MOX fuels with enrichment ranging from 1.0 to 6.0 wgt%. The plutonium isotopics for the two types of MOX cases are summarized in **Table 5** and the change in fuel density with temperature is given in **Table I-A** of the Appendix for all fuels types.

Table 5. Plutonium Isotopics (at.%).

Fuel	^{239}Pu	^{240}Pu	^{241}Pu	^{242}Pu
Reactor-Recycle MOX	45.0	30.0	15.0	10.0
Weapons-Grade MOX	93.6	5.9	0.4	0.1

Cladding and Moderator:

The cladding is taken to be pure zirconium, with no minor constituents of Zircaloy present, the moderator is the borated water, cladding and moderator densities are given in **Table I-B** of the Appendix.

5.3. Monte Carlo model

A series of MCNP(X) calculations have been performed for Doppler coefficient of reactivity using ENDF/B-VIII.0β6, ENDF/B-VIII.0β5, ENDF/B-VIII.0β4, ENDF/B-VII.1, ENDF/B-VII.0 and ENDF/B-VI.8 libraries. The geometry being a semi-infinite array of identical fuel pins of infinite length was used to calculate the effective multiplication factor at hot zero power and hot full power for each case. Small changes in the dimensions of the fuel

pins and cladding were made to account for thermal expansion. The obtained results for each fuel type with ENDF/B-VIII.0β6 are compared to those of ENDF/B-VIII.0β5, ENDF/B-VIII.0β4, ENDF/B-VII.1, ENDF/B-VII.0 ENDF/B-VI.8 and ENDF/B-V from the reference [4].

5.4. Results of Doppler Reactivity Defect Benchmarks

As we know, the Doppler coefficient of reactivity is generally negative and increases with uranium enrichment or MOX concentration and becoming consistently less negative as the enrichment or PuO_2 content increases. However, the change is much smaller for the MOX fuel than for the UO_2 fuel behaviour. In addition, the Doppler coefficient for heavy loadings of MOX fuel is significantly more negative than the Doppler coefficient for highly enriched UO_2 fuel. Natural uranium has been included in all three fuel types. In the MOX fuel, it is used just as a reference.

For UO_2 pin cells, it is clear from the results that the six versions of the cross-section libraries produce generally very similar values of keff parameter; statically the higher and lower values for keff are produced by ENDF/B-VII.1 and ENDF/B-VI.8 for every case, respectively. The obtained results using ENDF/B-VIII.0β6 are good. However, all the libraries produce very similar results for Doppler Coefficients. In addition, they produce also a very similar standard deviation (**σ**) for each case. The uranium fuel shows an increasing function to an asymptotic value (see **Fig.31** and **Fig. I-A**).

For Reactor-Recycle MOX pin cells, from the results it can be noted that ENDF/B-VIII.0β4, ENDF/B-VIII.0β5 and ENDF/B-VIII.0β6 produce the higher values for keff and ENDF/B-VI.8 the lower values. Moreover, all the libraries including ENDF/B-VIII.0β6 produce again a very similar Doppler Coefficients and standard deviations (**σ**), the deviations between σ are less than (1%). Moreover, ENDF/B-VI.8 and ENDF/B-VII.0 produce curves that have been slightly less negative with increasing PuO_2 content and ENDF/B-VIII.0β6 has a middle curve between the others when increasing PuO2 content (see **Fig.32** and **Fig. I-B**).

For Weapons-grade MOX pin cells, it can be observed that all the libraries produce very same values of Doppler Coefficients and (**σ**). The Doppler Coefficients have curves which are in the form of a shoulder for the variation between 1 w. % and 3 w. %. Furthermore, ENDF/B-VI.8 and ENDF/B-VII.0 libraries produce curves that are nearly flat. It is deduced that the results with ENDF/B-VIII.0β6 are good (see **Fig.33** and **Fig. I-C**).

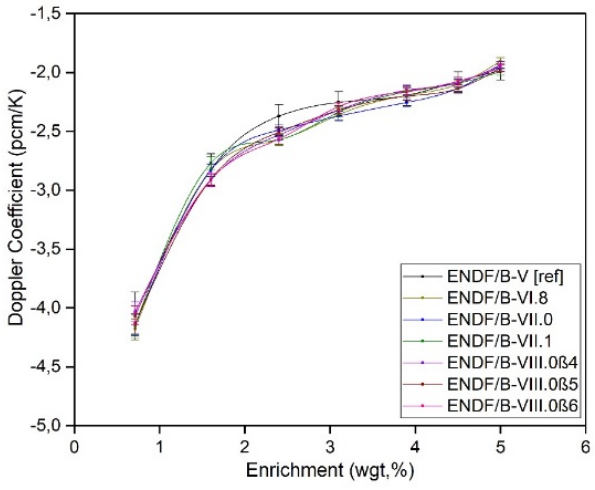

Fig.31. Doppler Coefficient for Normal and Enriched UO_2 Fuel.

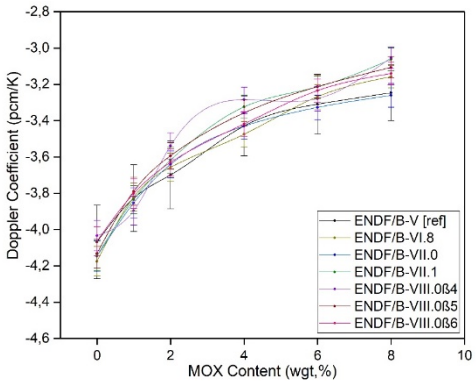

Fig.32. Doppler Coefficient for Reactor-Recycle MOX Fuel.

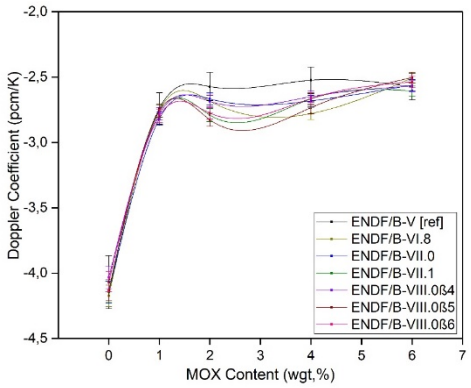

Fig.33. Doppler Coefficient for Weapons-Grade MOX Fuel.

6. Conclusion

In the current paper, Benchmark calculations have been performed for the recent release of ENDF/B VIII.0β6 data library, using the MCNP(X) Monte Carlo code and the latest version of the NJOY2016 processing code. The computations with ENDF/B-VI.8, ENDF/B-VII.0 ENDF/B-VII.1, ENDF/B-VIII.0β4 and ENDF/B VIII.0β5 libraries have also been made for determining the improvements of the new library. The subjects of the calculations were criticality safety, shielding, and Doppler Reactivity Defect benchmarks.

The performance of the new library for the criticality benchmarks in combination with NJOY2016 and MCNP(X), is shown to be good agreement with the benchmark values. The result for the U233-SOL-INTER-001-case-1 benchmark based on Beryllium has been improved since the obtained value is very close to that of ENDF/B-VII.0 and the difference is less than 200 pcm. For most other benchmarks, the results are also in good agreement with the published values. For shielding benchmarks, we benchmarked ENDF/B VIII.0β6 with the TOF Oktavian experiments. Generally, it can be concluded that ENDF/B VIII.0β6 is improved in some cases for each specific energy region by comparing with the other libraries. However, small differences in values exist between the libraries in the majority of applications. Largest differences can likely be due to original nuclear data in many cases. Also, there are strong deviations between computed and benchmark values in some cases. The behaviour of the Doppler coefficients is in fact similar in almost all cases. The coefficients and the standard deviation (**σ**) from the ENDF cross-section libraries including ENDF/B VIII.0β6 are statistically indistinguishable. However, differences can be observed in the values for keff'. In other terms, the keff parameter does not much matter when it is used to compute the Doppler coefficients.

To conclude, the new ENDF/B VIII.0β6 library has been demonstrated much better performance than the previous ENDF evaluations for most applications, except in some cases and in some energy ranges this library must be further improved.

Acknowledgment

The authors would like to express many thanks to Nuclear Reactor and Nuclear Security Group (PRESN) especially the professor A. CHETAINE for valuable support to the writing of this paper and their great scientific advices. Moral supports from colleagues on PRESN are greatly appreciated.

APPENDIX I. Doppler Reactivity Defect: Benchmark specifications and results.

The densities and isotopic concentrations [13] for the benchmarks are provided in **Table I-A** and **Table I-B.**

The keff results obtained using MCNP(X) are presented in **Fig I-A** to **I-C**.

Table I-A. Fuel density for Different Temperatures.

		Density of fuel (in g/cc)
UO2 fuels	600K	10.3390
	900K	10.3120
Reactor-Recycle MOX fuels	600K	10.3376
	900K	10.3106
Weapons-Grade MOX fuels	600K	10.3376
	900K	10.3106

Table I-B. Atomic Densities for Cladding and Water at 600 K with 1400 PPM of Boron.

Materials	Isotope	Number density (atoms/b-cm)
Cladding	Zr-nat	4.21838E-02
Moderator	^{1}H	4.42326E-02
	^{10}B	1.02133E-05
	^{11}B	4.11098E-05
	^{16}O	2.21163E-02

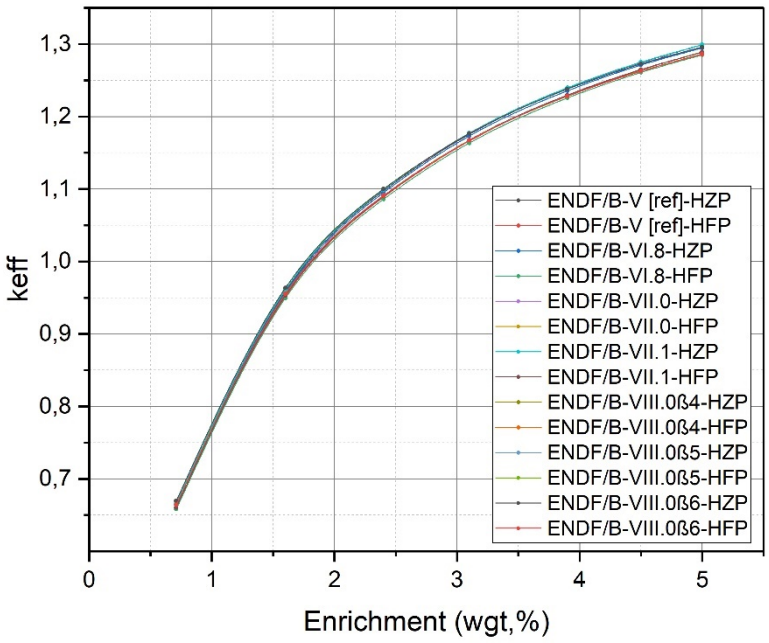

Fig. I-A. keff results for UO2 Pin Cells.

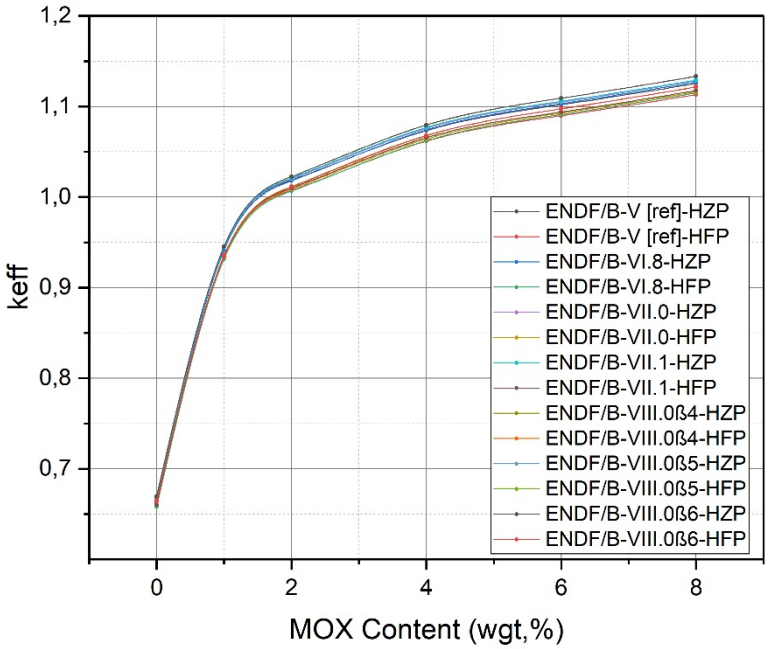

Fig. I-B. keff results for Reactor-Recycle MOX Pin Cells.

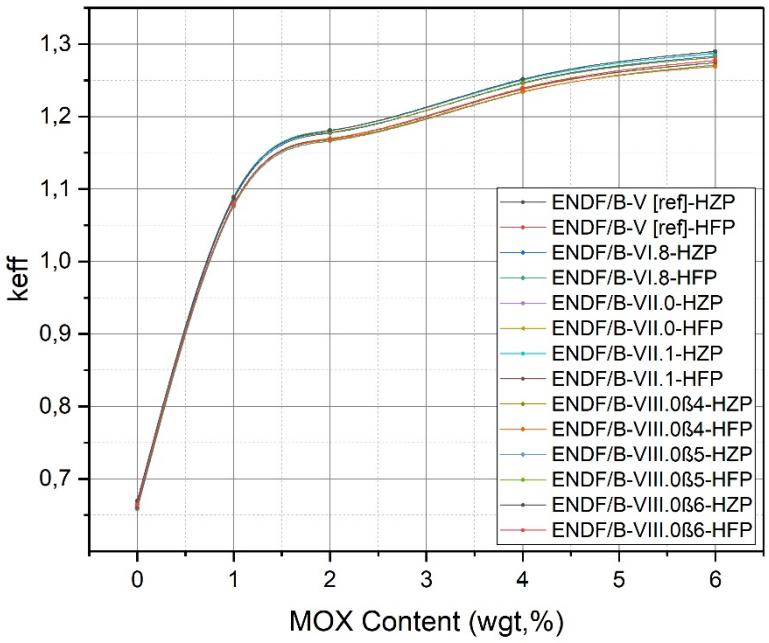

Fig. I-C. keff results for Weapons-grade MOX Pin Cells.

References

[1] ENDF/B-VIII.0beta6 US Evaluated Nuclear Data Library [Internet] 2017. Available from: https://ndclx4.bnl.gov/gf/project/endf/

[2] NEA/NSC/DOC (95)03/IJ.B. Briggs (Ed.), International Handbook of Evaluated Criticality Safety Benchmark Experiments, Nuclear Energy Agency, Paris, France, September 2004.

[3] https://www-nds.iaea.org/fendl2/validation/benchmarks/jaerim94014/oktavian/n-leak/

[4] R. D. Mosteller, ENDF/B-V, ENDF/B-VI, and ENDF/B-VII.0 Results for the Doppler-Defect Benchmark, LA-UR-07-0922, Join international Topical Meeting on Mathematics & Compilation and Supercomputing in Nuclear Applications (M&C + SNA 2007) Monterey, California, April 15-19, 2007.

[5] J.S. Hendricks, G.W. McKinney, M.L. Fensin, M.R. James, R.C. Johns, J.W. Durkee, J.P. Finch, D.B. Pelowitz, L.M. William Johnson, F.X. Gallmeier, MCNPX 2.6.0 Extensions LA-UR-08-2216, National Laboratory and Oak Ridge National Laboratory, Los Alamos, April 11, 2008

[6] ENDF/B-VIII.0beta5 US Evaluated Nuclear Data Library [Internet] 2017. Available from: https://ndclx4.bnl.gov/gf/project/endf/

[7] R.E. MacFarlane, D.W. Muir, R.M Boicourt, A.C. Kahler, J.L. Conlin, The NJOY Nuclear Data Processing System, Version 2016 LA-UR-17e20093 [Internet]. Los Alamos National Laboratory, December 19, 2016. Available from: https://njoy.github.io/NJOY2016/

[8] M. Mattes, J. Keinert, Thermal neutron Scattering Data for the Moderator Materials H2O, D2O and ZrHx in ENDF-6 Format and as ACE Library for MCNP(X) Codes, INDC(NDS)-0470, 2005.

[9] P. Balaji, D. Buntinas, R. Butler, A. Chan, D. Goodell, W. Gropp, J. Krishna, R. Latham, E. Lusk, G. Mercier, R. Ross, R. Thakur, MPICH2 Installer's Guide, Mathematics and Computer Science Division, Argonne National Laboratory, October 8, 2012.

[10] S.C. van der Mark, Criticality Safety Benchmark Calculation with MCNP-4C3 Using JEFF-3.1 Nuclear Data, Petten, October 7, 2005.

[11] K. Ouadie, C. Abdelouahed, J. Abdelhamid, D. Abdelaziz, and S. Abdelmajid, "Processing and benchmarking of evaluated nuclear data file/b-viii.0β4 cross-section library by analysis of a series of critical experimental benchmark using the monte carlo code mcnp(x) and njoy2016," Nucl. Eng. Technol., 2017.

[12] C. Ichihara, I. Kimura, S. A. Hayashi, J. Yamamoto, and A. Takahashi, "Measurement of leakage neutron spectra from a spherical pile of zirconium irradiated with 14mev neutrons and validation of its nuclear data," J. Nucl. Sci. Technol., vol. 40, no. 6, pp. 417–422, 2003.

[13] R. D. Mosteller, "The Doppler-defect benchmark: overview and summary of results," Jt. Int. Top. Meet. Math. Comput. Supercomput. Nucl. Appl. (M&C + SNA 2007), pp. 1–13, 2007.